Theoretical bases of modeling of nanostructures formed from the gas phase

A. Vakhrushev, A. Fedotov and V. Golubchikov

***Abstract*—**The mathematical model of condensation processes of nanoparticles from a gas phase is submitted for nanoaerosol and nanocomposite systems. The determination method of mechanical and structural nanoparticles properties is proposed. Theoretical analysis of composites elastic characteristics including nanoparticles is carried out. Calculation results of metals nanoparticles formation at vacuum evaporation and condensation are given. Numerical and structural properties of forming nanoobjects is examined. Dependences of structural behavior for nanoobjects and composites on basis of its are obtained. Research is carried out for the processes of aerosol and nano composite systems.

***Keywords*—** nanoparticles, simulation, molecular dynamics, strength properties, nanocomposites, nanoaerosol.

I. Introduction

The study of the processes of interaction and the formation of substances at the nanoscale allows obtaining new functionality materials, as well as keeping track of their properties and structural features to determine their molecular structure. In this situation the question of formation of nanoparticles, as well as obtaining homogeneous nano-dispersed mixtures of these and other nanoelements for making nanocomposites with homogeneous and stable in terms of the characteristics of the material is given considerable interest. This is due to the fact that the physical-mechanical, chemical and other properties of nanoparticles greatly and typically depend nonlinearly on the nanoparticle size [1, 2].

The use of nanocomposites and nanoaerosoles is prospectively in environmental terms. The nanoparticles of titanium oxide and cerium may be dangerous for a person to decompose nitrogen oxides and carbon contained in automobile exhaust. Scientists have conducted research on the treatment of environmental media from contamination by means of nano ingredients. Japanese authors [3] have developed a new nanomaterial which includes a porous oxide, manganese gold particles grown therein. Made substance effectively removes volatile organic compounds as well as sulfur and nitrogen oxides from air at room temperature.

Composites of nanoparticles are widespread in medicine and pharmacy [4], in which the nanoparticles targeted on drug delivery to cells and protein bodies as well as on artificial muscles and bones. Scientists from the Research Center of American Dental Association in cooperation with the National Institute of Standards and Technology were able to demonstrate that nanotechnology can create sealing material, which is more durable than any previously known therapeutic fillers, and thus it is more effective in preventing repeated failure of a tooth [5]. Authors Quentin le Masne de Chermont, Corinne Chaneac et al found that some of the nanoparticles containing a metal may be used for visualization of cancer cells [6]. A similar diagnostic effect of heart disease, cancer, and neurodegenerative diseases, but on the basis of nanoparticles containing esters per oxalates and fluorescent dyes, the researchers have made the Georgia Institute of Technology Dongwon Lee, Sirajud Khaja, Juan C. Velasquez-Castano et al [7]. A team of scientists from the universities of Indiana and Texas have developed the expertise and learned to destroy the tumor cells [8]. Gold nanoshells were injected into the diseased organ, and then delivered to the cancer cells, monocytes and macrophages (immune cells) and under the influence of irradiation led to the elimination of poor quality units.

Metal nanoparticles have attracted the interest of many researchers because of its functional features [9]. Depending on the method of synthesizing nanoparticles of their shape can be varied. Depending on the method of synthesizing nanoparticles of their shape can be varied. There have been cases of synthesis of nanostructures as nanospiraley obtained by the sol-gel method [10], nanofilms deposited by pulsed laser deposition on a substrate and chaotic multicomponent formations formed by dispersing [11]. Nanoparticles are widespread because the spherical shape of a balanced energy state.

Currently, nanotechnology is working closely with many sciences, disciplines and industries. For nanocomposite materials it is necessary to provide uniform and stable in terms of material characteristics, as even a slight variation of the composition, in any local area, could lead to a sharp decrease in the mechanical properties of the nanocomposite that caused the nanodefects under operational loads and significantly

The work was supported by RFBR (project №13-08-01072 a), RSF (project № 15-19-10002), the Kalashnikov Izhevsk State Technical University (S. task 2014/45-1239) and the JSC ″Nord″.

A. V. Vakhruchev is with Kalashnikov Izhevsk State Technical University, 7 Studencheskaya street, Izhevsk, Russia, 426069 (corresponding author to provide phone: +7-3412-214583; e-mail: vakhrushev-a@yandex.ru).

A. Yu. Fedotov is with Institute of Mechanics Ural Branch of Russian Academy of Science, 34 T. Baramzinoy street, Izhevsk, Russia, 426067 (e-mail: alezfed@gmail.com).

V.B. Golubchikov is with Join Stocks Company ″Nord″, 1 Levchenko, Perm, Russia, 614990 (nord59r@mail.ru)

reduce product reliability. Experimental study of the mechanisms of formation of nanoparticles is technically difficult and time consuming task, due to the small size of the data objects. Simulation is an alternative and promising way to study the mechanisms of formation of nano-objects and it is very topical. Determination of physical, mechanical, structural and quantitative characteristics of the size and shape of the nanoparticles formed in order to determine the properties of nanocomposite materials based on its is important. The aim of work was to study the specific processes, their parameters and their optimization by means of mathematical modeling.

II. Problem Formulation

Simulation of the formation of nanoparticles, nanocomposites, and nanoaerosoles were carried out by molecular dynamics, which is based on the numerical solution of differential equations of motion Newton for each atom with an initial assignment of velocities and coordinates:

$$m_i \frac{d^2 \overline{\mathbf{r}}_i(t)}{d t^2} = -\frac{\partial U(\overline{\mathbf{r}}(t))}{\partial \overline{\mathbf{r}}_i(t)} + \overline{\mathbf{F}}\left(\overline{\mathbf{r}}(t), t\right), \qquad (1)$$

$$t = 0, \overline{\mathbf{r}}_i\left(t_0\right) = \overline{\mathbf{r}}_{i0}, \frac{d\overline{\mathbf{r}}_i\left(t_0\right)}{dt} = \overline{\mathbf{V}}_i\left(t_0\right) = \overline{\mathbf{V}}_{i0}, \qquad (2)$$

where $i = 1, 2, .., K$, K – the number of atoms that formed nanosystem; m_i – the mass of the i-th atom; $\overline{\mathbf{r}}_{i0}, \overline{\mathbf{r}}_i(t)$ – the initial and current radius vector of the i-th atom, respectively; $U(\overline{\mathbf{r}}(t))$ – the potential energy of the system; $\overline{\mathbf{V}}_{i0},, \overline{\mathbf{V}}_i(t)$ – the initial and current speed of the i-th atom, respectively; $\overline{\mathbf{r}}(t) = \left\{\overline{\mathbf{r}}_1(t), \overline{\mathbf{r}}_2(t), .., \overline{\mathbf{r}}_K(t)\right\}$ – shows the dependence of the location of all the atoms system, $\overline{\mathbf{F}}\left(\overline{\mathbf{r}}(t), t\right)$ – an external force.

Simulation of the formation of nanoaerosol systems was carried out in a representative volume of calculated with periodic boundary conditions. The computational region for the solution of the above problem is shown in Fig. 1. A more detailed statement of the problem and the simulation methodology described in earlier papers [12-15].

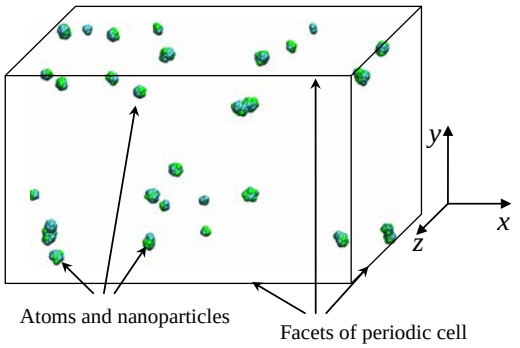

Fig. 1. The computational region in the simulation of nanoaerosol systems formed from the gas phase

The dynamic observation of the elastic properties of the nanocomposites were implemented as follows. Matrix composites with nanoinclusions was subjected shear or tensile strain (Fig. 2). Here, as the input parameters of the system set the speed of deformation. After effect on the nanosystem its atoms begin to rebuild. The main mechanical and physical properties were calculated.

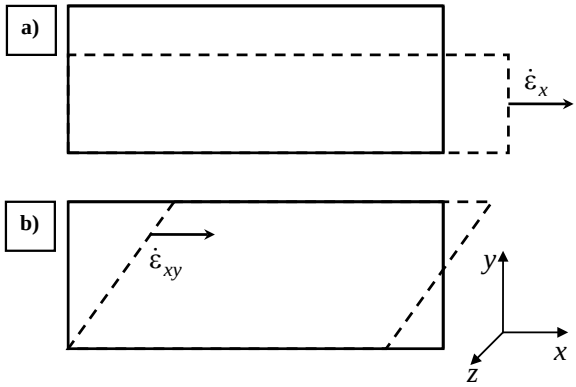

Fig. 2. Scheme nanocomposite stretching deformation (a) and shear (b)

The potential energy of the system (1) is determined by the modified embedded-atom method (MEAM). The theory of MEAM is derived by using density functional theory (DFT). DFT method is currently considered the most recognized approach to the description of the electronic properties of solids. In embedded-atom method complete electron density is a linear superposition of spherically averaged functions. This disadvantage is eliminated in the modified embedded atom method.

The method MEAM energy of the system is written in the form:

$$E = \sum_i \left(F_i\left(\frac{\overline{\rho}_i}{Z_i}\right) + \frac{1}{2}\sum_{j \neq i} \varphi_{ij}\left(R_{ij}\right)\right), \qquad (3)$$

where E – atomic energy i; F_i –function for atom i, embedding in the electron density $\overline{\rho}_i$; Z_i – the number of nearest neighbor atoms i reference in its crystalline structure; φ_{ij} – pair potential between atoms i, j, located at a distance R_{ij}.

In MEAM $F(\rho)$ determined as a function of embedding

$$F(\rho) = AE_c \rho \ln \rho, \qquad (4)$$

where A – controlled variable; E_c – binding energy.

Pair potential between atoms i, j is determined by

$$\varphi_{ij}(R) = \frac{2}{Z_i}\left\{E_i^u(R) - F_i\left(\frac{\overline{\rho}_i^0(R)}{Z_i}\right)\right\}, \qquad (5)$$

where $\overline{\rho}_i^0$ – electron density.

The total electron density at the dive includes angular dependence and written in the form:

$$\overline{\rho} = \rho^{(0)} G(\Gamma). \quad (7)$$

There are many types of functions $G(\Gamma)$ [16]:

$$G(\Gamma) = \sqrt{1+\Gamma},\ G(\Gamma) = e^{\frac{\Gamma}{2}}, \quad (8)$$

$$G(\Gamma) = \frac{2}{1+e^{-\Gamma}},\ G(\Gamma) = \pm\sqrt{|1+\Gamma|}. \quad (9)$$

The function Γ is calculated according to the formula:

$$\Gamma = \sum_{h=1}^{3} t^{(h)} \left(\frac{\rho^{(h)}}{\rho^{(0)}} \right)^2, \quad (10)$$

where $h = 0-3$, correspond to *s, p, d, f* symmetry; $t^{(h)}$ – weight multipliers; $\rho^{(h)}$ – values, determining the deviation of the distribution of the electron density distribution of a perfect crystal of the cubic system $\rho^{(0)}$:

$$s(h=0): \rho^{(0)} = \sum_i \rho^{a(0)}(r^i), \quad (11)$$

$$p(h=1): \left(\rho^{(1)}\right)^2 = \sum_\alpha \left[\sum_i \rho^{a(1)}(r^i) \frac{r_\alpha^i}{r^i} \right]^2, \quad (12)$$

$$d(h=2): \left(\rho^{(2)}\right)^2 = \sum_{\alpha,\beta} \left[\sum_i \rho^{a(2)}(r^i) \frac{r_\alpha^i r_\beta^i}{r^{2i}} \right]^2 - \frac{1}{3} \sum_i \left[\sum_i \rho^{a(2)}(r^i) \right]^2, \quad (13)$$

$$f(h=3): \left(\rho^{(3)}\right)^2 = \sum_{\alpha,\beta,\gamma} \left[\sum_i \rho^{a(3)}(r^i) \frac{r_\alpha^i r_\beta^i r_\gamma^i}{r^{3i}} \right]^2. \quad (14)$$

Here $\rho^{a(h)}$ – radial functions that represent a decrease in the contribution of distances r^i, superscript *i* indicates the nearest atoms, α, β, γ – summing the codes for each of the three possible directions. Finally, the individual contribution is calculated according to the formula:

$$\rho^{a(h)}(r) = \rho_0 e^{-\beta^{(h)}\left(\frac{r}{r_e}-1\right)}. \quad (15)$$

III. Calculation Technique of Elastic Properties of Composite Materials

The main deformation characteristics of objects include effective bulk modulus of the material k and the effective shear modulus μ. If necessary, transition is possible from this values to Young's modulus E and Poisson's ratio ν according to (16). Backward calculations are possible too.

$$E = \frac{9k\mu}{3k+\mu},\ \nu = \frac{3k-2\mu}{2(3k+\mu)}. \quad (16)$$

When working with composites and studying its properties, bulk material generally been considered the two components: the matrix and inclusions. The matrix is macro material forming the primary composite structure. The inclusions are some additives in the matrix to refine and improve its mechanical or other characteristics. Deformation properties of the matrix are compatible with the bulk material. They are usually taken from reference books. The strength properties of the inclusions is much more difficult to define. Either experimental data or theoretical methods are used when calculating them. In our case as the inclusions are nanoparticles. To determine the deformation properties and dependencies of the model of the elastic "equivalent" element tensile concentrated forces described above is used.

It is known from previously conducted studies [17] and the effect of the Hall-Petch, the effective bulk modulus and effective shear modulus of nano-objects is not a linear function of their size. Generalized dependence of these quantities can be written in the form of expressions:

$$k_I = \begin{cases} A\left(\frac{d}{d_0}\right)^B, \text{if } d \le d_0 \\ k_{I0}, \text{if } d > d_0 \end{cases} = \begin{cases} A\left(\overline{d}\right)^B, \text{if } \overline{d} \le 1 \\ k_{I0}, \text{if } \overline{d} > 1 \end{cases}, \quad (17)$$

$$\mu_I = \begin{cases} M\left(\frac{d}{d_0}\right)^L, \text{if } d \le d_0 \\ \mu_{I0}, \text{if } d > d_0 \end{cases} = \begin{cases} M\left(\overline{d}\right)^L, \text{if } \overline{d} \le 1 \\ \mu_{I0}, \text{if } \overline{d} > 1 \end{cases}, \quad (18)$$

where k_I, μ_I – the effective bulk modulus and effective shear modulus of inclusions, $d, \overline{d}$ – actual and relative sizes of the nanoparticles, k_{I0}, μ_{I0} – the effective bulk modulus and effective shear modulus of volume material, which consists of inclusions, d_0 – the diameter of the nanoobjects in which they cease to depend on the elastic properties of the size, A, B, M, L – some of the coefficients, calculated empirically. Having determined the values of the coefficients A, B, M, L, it is possible to calculate the strength parameters of nanostructures of all sizes.

In some cases, it is convenient to use dimensionless or relative deformation characteristics of the inclusions. Dimensionless made in relation to macro properties of material k_{I0} and μ_{I0}:

$$\bar{k}_I = \frac{k_I}{k_{I0}} = \begin{cases} \frac{A}{k_{I0}}\left(\bar{d}\right)^B, \text{if } \bar{d} \le 1 \\ 1, \text{if } \bar{d} > 1 \end{cases}, \quad (19)$$

$$\bar{\mu}_I = \frac{\mu_I}{\mu_{I0}} = \begin{cases} \frac{M}{\mu_{I0}}\left(\bar{d}\right)^L, \text{if } \bar{d} \le 1 \\ 1, \text{if } \bar{d} > 1 \end{cases}. \quad (20)$$

With a known mechanical parameters and dependencies for inclusions in the form of nanoparticles, the calculation of similar properties of the composite material performed based on of formulas and techniques from [18]. Model of the medium with low volume fraction of spherical inclusions is expressed by the following relationships:

$$\bar{k} = \frac{k}{k_M} = 1 + \frac{\left(\frac{k_I}{k_M} - 1\right)c}{1 + \left(k_I - k_M\right)\Big/\left(k_M + \frac{4}{3}\mu_M\right)}, \quad (21)$$

$$\bar{\mu} = \frac{\mu}{\mu_M} = 1 - \frac{15\left(1-\nu_M\right)\left[1-\left(\mu_I/\mu_M\right)\right]c}{7 - 5\nu_M + 2\left(4-5\nu_M\right)\left(\mu_I/\mu_M\right)}, \quad (22)$$

where $k, \bar{k}$ – the dimension and the relative effective bulk modulus of the composite, $\mu, \bar{\mu}$ – the dimension and the relative effective shear modulus of the composite, c – the volume fraction of the nanoparticles included in the composite material, k_M, μ_M – the deformation parameters of the matrix.

IV. Research Results of Formation of Nanoparticles Used for Feeding the Plant from the Gas Environment

The process of mineral salts adding as nanoparticles in the pores of the plant functions is as followed [19, 20]. Initially fertilizers together with combustible material pressed into a tablet form (Fig. 3.1), the tablet is ignited, leading to a transition of minerals in the gaseous state (Fig. 3.2), in the gas phase is the formation of nanoparticles, which subsequently penetrate into the plants and feed them (Fig. 3.3).

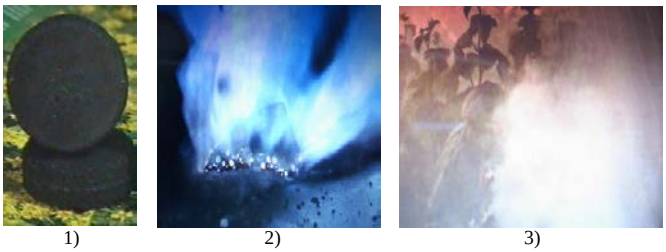

1) 2) 3)

Fig. 3. The steps of adding mineral salts, 1) the tablet from mineral salts and combustible material, 2) combustion tablets 3) plant nutrition

According to studies, the gas composition after burning mineral tablet comprises more than 20 types of molecules. The main elements of the gas mixture and the mass fractions in ascending order are shown in Fig. 4. Analysis of the graph shows that most of the mass of the gas molecules occupy the oxygen and carbon dioxide, among the mineral salts of potassium carbonate has the advantage – K_2CO_3. Mass fractions of elements in the row after the nitrogen and minor amount not exceeding 5 % of the total weight of the gas mixture.

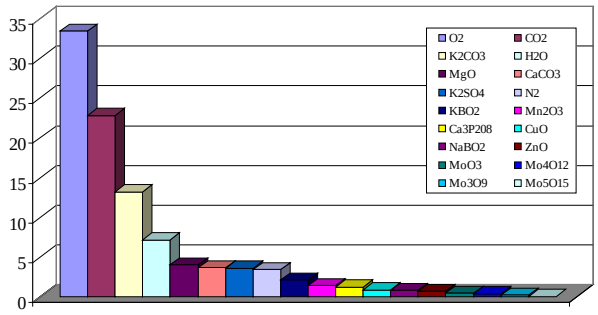

Fig. 4. Mass fraction of the gas mixture

Based on the mass fractions of elements as the ratio to the molar mass can be calculated fraction of molecules in the gas phase. For cells, the most frequently encountered in gas phase, the proportion of the number of molecules is as follows: O_2 – 43.24 %, CO_2 – 21.62 %, H_2O – 16.47 %, N_2 – 5.41 %, MgO – 4.13 % and K_2CO_3 – 3.95 %. The proportion of the number of molecules for the other elements is the amount of 5.18 %, of which the maximum value corresponds to the molecules Ca_2CO_3 – 1.51 %. A small number of molecules, most of the elements of the gas phase allows a high degree of reliability does not take into account their impact on the formation of nanoparticles. Thus, to simulate the formation of atomic and molecular motion and condensation mineral nanoparticles is sufficient to consider only six basic types of molecules O_2, CO_2, H_2O, N_2, MgO and K_2CO_3. The total number of atoms of the simulated system was chosen $N = 9000$ atoms. In accordance with the total number of atoms and the proportion of number of molecules of each element of the system studied was determined the number of molecules of each type.

To calculate the equilibrium configuration of the molecules of the starting materials was used first-principles method. The basis was chosen basis 6-31G*, satisfying a wide class of chemical elements. Geometry optimization of molecules made using the conjugate gradient method Fletcher-Reeves. As a result, the calculation method of the first principles determined by the equilibrium bond lengths in molecules, the equilibrium values of the angles and dihedral angles, atomic charges of the molecules.

For each of the six basic types of molecules, forming a gas phase and in Fig. 4, we calculated the equilibrium configuration. Appearance of molecules with optimized structure is shown in Fig. 5: 1) for a molecule of carbon dioxide, 2) for the water molecule and 3) a molecule of potassium carbonate. Molecules magnesium oxide, nitrogen

and oxygen have a linear structure, and differ only in the type of atoms in a molecule, number and length of connections.

Simulation the formation of composite nanoparticles of potassium and magnesium oxide was carried out in two stages. At the first stage the system was heated to 600 K for a uniform distribution of all elements of the initial gas mixture.

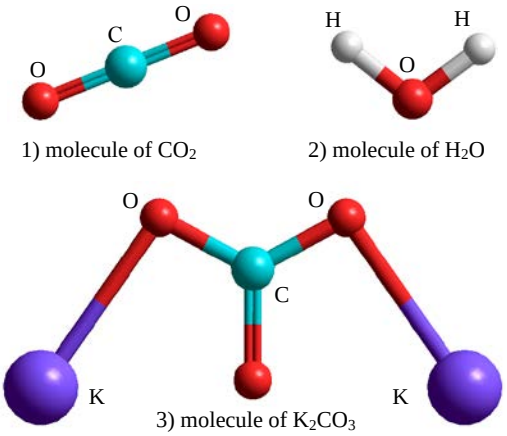

1) molecule of CO_2 2) molecule of H_2O

3) molecule of K_2CO_3

Fig. 5. An example of the equilibrium configuration of molecules

The second stage corresponds condensation step of atoms, molecules and nanoparticles at normal temperature (300 K). The duration of the first and second stages was 16 ns and 6984 ns, respectively. The duration of the heating stage is defined by uniform mass distribution of the settlement amount, which is an indicator of compositional homogeneity of the mixture. Irregularities presented at the initial time in the distribution of weight, were decreased with time, and in the future do not exceed 5 %. Appearance formed composite nanoparticles is shown in Fig. 6.

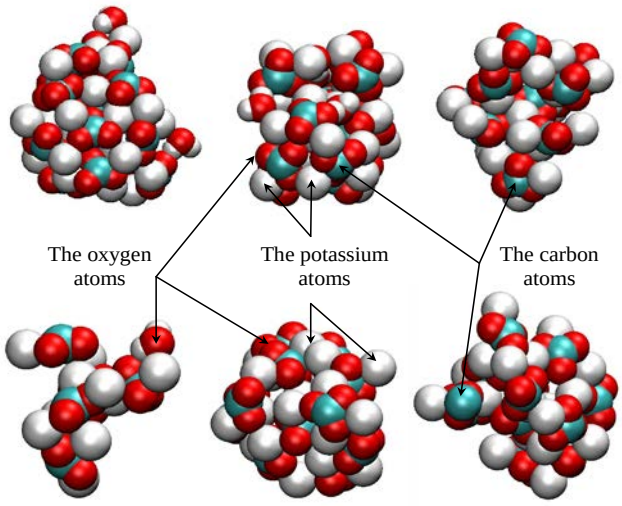

Fig. 6. Image of composite nanoparticles

The obtained nanoparticles have a different structure and shape. However, the internal structure is the same: the nanoparticles are solid within the cavities in the structure are not observed. The simulation showed that in the period up to 16 ns, correspond to the duration of the heating phase, the association of molecules in the nanoparticles is observed. In the cooling step are actively participating in a condensation molecule potassium carbonate, less intensive water molecules are grouped and magnesium oxide.

The distribution of the nanoparticles on the molecular weight fraction of potassium carbonate given for the time of 110 ns in Fig. 7 describes the chemical composition of the composite nanoparticles formed. Most of nanoparticles (76 % of the total) consists of more than 75 % of the mass of molecules K_2CO_3. The molecules of potassium carbonate have considerable weight and are the centers of condensation of nanoparticles. However, in the gas mixture, there is formation of nanoparticles (20 % of total), which structure does not include K_2CO_3. These nanoparticles consist primarily of water molecules. Molecules of carbon dioxide, nitrogen and oxygen in the composition of the nanostructures and practically includes all over modeling systems are in a gaseous state. Such an effect, according to the authors, because the molecules CO_2, O_2 and N_2 are present in the volume of investigation as components of a mixture of air and combustion products, which under normal conditions are not clustered.

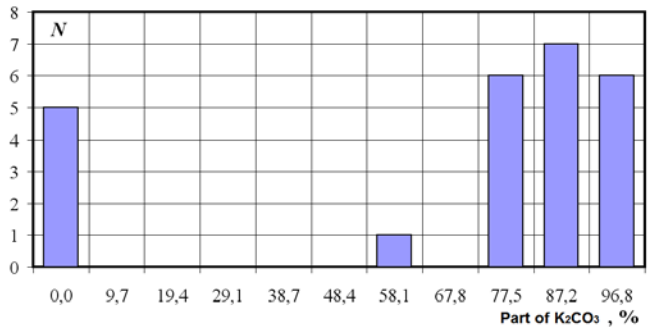

Fig. 7. The distribution of nanoparticles on a mass fraction of K_2CO_3 molecules

Based on the size distribution of the nanoparticles at each time point was determined by the dynamics of the average diameter of the nanoparticles shown in Fig. 8 (left scale). The dependence of the number of nanoparticles per unit volume of the time is shown in Fig. 8 (right scale) and the ordinate is logarithmic scale used. The initial moments of time correspond to a significant increase in the number of nanoparticles, as occurred at the beginning stages of cooling and condensation. In subsequent times the number of nanoparticles varies slightly. This behavior is explained by the number of nanoparticles a small amount of condensation nuclei, which are molecules of potassium carbonate. The number of molecules of K_2CO_3 with respect to the total number of molecules is small, so the formation of a significant number of nanoparticles in the test volume is observed.

Data from molecular dynamics simulation were used as the primary method for the motion of the particles. The method of the particles was carried out modeling of nanosystems 100-7000 ns time steps, the results of which have been calculated parameters and properties of composite nanoparticles and the curves change in the average diameter and number of

nanoparticles per unit volume. The times of 0-100 ns in Fig. 8 correspond to the initial stage of formation of composite nanoparticles by the method of molecular dynamics. Evidence suggests that the growth rate of the size of the nanostructures decreases with time. The weight of the formed nanoparticles increases, the mobility decreases, which leads to reduction in the number of nanoparticles per unit volume.

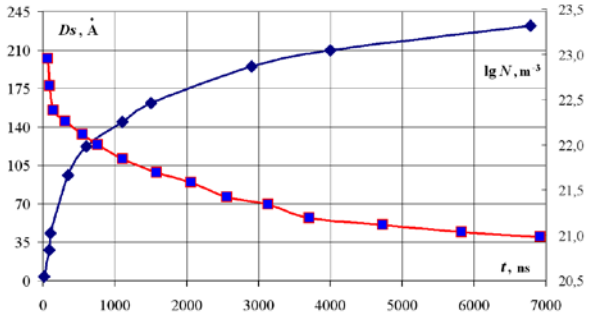

Fig. 8. The change in the average diameter and the total number of nanoparticles per unit volume

When we use the motion of the particles was carried out increasing the spatial scale by combining several nanosystems mirroring settlement areas. The increase in the computational cell produced repeatedly, and the amount of the study area increased by more than 100 times, compared to stage molecular dynamics simulation. Application the method of particles allowed to carry out an analysis of the formation of composite nanoparticles in large time scales. By reducing the number of the objects in the system (in the particle method considered only formed nanoparticles, the impact of the gas phase is determined by the size of the random force) was obtained increases in computing performance compared with molecular dynamics simulation.

V. Research Results of Nanoaerosol Fire-Extinguishing

Let us consider the results of calculations of the processes of nanoparticle condensation during operation of the of the aerosol fire extinguisher [21, 22]. The mix in the aerosol fire extinguisher includes 7 basic components. The mass fractions of these components are presented in Fig. 9. The gas phase mainly consists of the molecules of nitrogen and carbonic gas. The molecules of potassium carbonate (K_2CO_3) consitute the basic component of the solid phase.

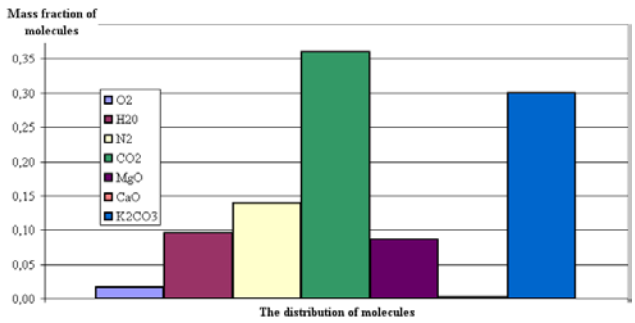

Fig. 9. Mass fractions of aerosol components

For each of seven types of the molecules forming the gas phase shown in Fig. 9 the equilibrium configurations have been calculated. As an example, the appearance of a molecule of water with optimized geometry is shown in Fig. 10.1, and the appearance of a molecule of potassium carbonate with optimized geometry is shown in Fig. 10.2. Figure 10.2 also contains the surface of electrostatic potential of a molecule of potassium carbonate, with the green color corresponding to the positive potential +0.1 eV and the purple one, to the negative potential -0.1 eV.

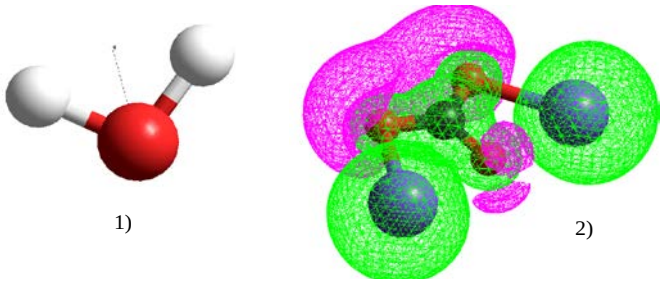

1) 2)

Fig. 10. The structure of water molecules 1) and potassium carbonate 2)

Usually, in real experiments the molecular system exchanges energy with the environment. For calculating such power interactions, special algorithms – “thermostats” are used. Use of a thermostat allows one to carry out calculation of molecular dynamics at a constant temperature of the environment or to change it by a certain law. With this aim, the stage of condensation of an aerosol mix after active burning was considered. Therefore the temperature of the system modeled was kept slightly above the normal one (at a level of 310 K) due to the use of a Berendsen thermostat.

Another important point is stabilization of the nanosystem pressure. Use of the “barostat” algorithms makes it possible to model the behavior of the system at constant pressure. The most simple of them is the Berendsen barostat in which the pressure is kept stationary by means of scaling the computational cell. The positions of particles in systems are modified on each time step according to the factor of barostat scaling.

The process of condensation of molecules into nanoparticles is reflected by the dynamics of change in the relative weight of grouped molecules (Fig. 11). The line with square symbols corresponds to the relative weight of condensed K_2CO_3 molecules, with rhombic symbols, to H_2O, with triangular symbols, to MgO, and with round symbols, to N_2.

Curves describing the changes in the amount of condensed molecules of oxygen and calcium oxide were not obtained, since the molecules of these substances were in a gaseous state. Carbonic gas and nitrogen were condensed into nanoparticles least actively. Such an effect points to the fact that the CO_2, O_2, and N_2 molecules were present in the volume investigated as compound components of the mix of air with combustion products which under normal conditions do not

unite into nanoparticles. The quantity of the molecules of calcium oxide in the volume modeled is insignificant, which corresponds to their mass fraction in Fig. 9. Therefore, they constitute a part of the nanoparticles formed in small quantity. The analysis of Fig. 11 shows that the association of molecules into nanoparticles during the entire stage of condensation is observed. The molecules of potassium carbonate participate in condensation most actively. They have the greatest weight and are the centers of condensation. Because of the small values of the forces of interaction, the unstable nanoparticles can lose molecules from their structure, and break up into nanostructures smaller in size.

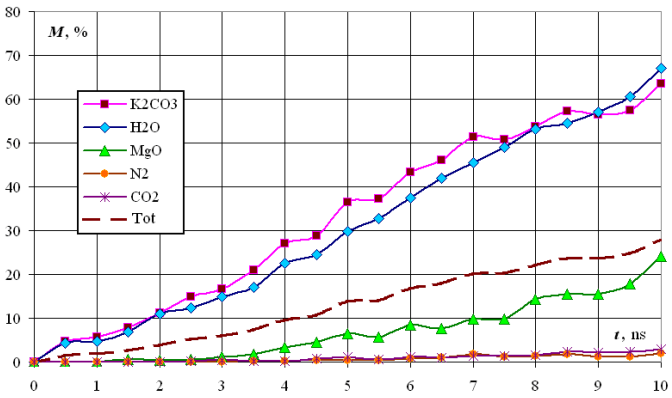

Fig. 11. Change in the mass fraction of nanosystem molecules grouped into nanoparticles

In Fig. 12, the change in the number of nanoparticles in a unit volume at the logarithmic scale is given. The analysis of Fig. 12 shows that the amount of nanoparticles is stably reduced due to the merging and association of nanostructures. The asymptotic behavior of a curve is observed: the quantity of nanoparticles in a unit volume varies more slowly eventually.

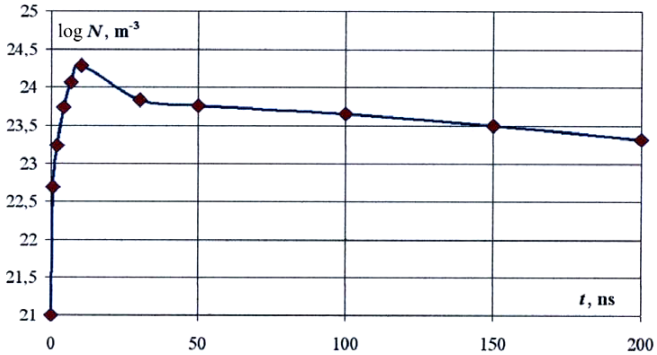

Fig. 12. Change in the number of nanoparticle in a unit volume obtained in modelling by the molecular dynamics and mesodynamics method

The weight of the nanoparticles formed grows, the mobility decreases, which causes a decrease in the number of nanoparticles in a unit volume. In using the mesodynamics method, the increase in the spatial scale of the nanosystem because of association of several symmetrically displayed computational areas was obtained. It has allowed carrying out an analysis of the processes of nanoparticle formation at big time scales. The mesodynamics considers only generated nanoparticles; the influence of the gas phase is determined by the magnitude of casual forces. Therefore, a substantial increase in the computing productivity has been obtained in comparison with the molecular dynamics modeling due to reduction in the number of objects in the system.

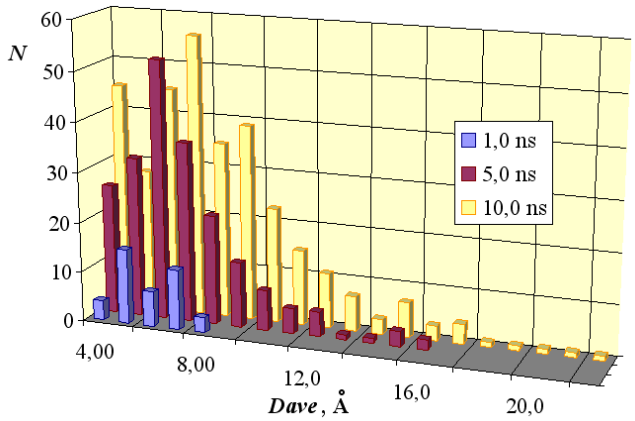

Fig. 13. Distribution of nanoparticle sizes at various moments of time

The size distribution of nanoparticles in various moments of time is presented in Fig. 13. For the size of a nanoparticle, the maximal distance between two atoms of a nanoparticle was taken. In the figure, the dependences the amount of nanoparticles on the diameter in 1, 5, and 10 ns are given. At the beginning of the process of condensation small nanoparticles are formed. By the moment of 1 ns the number of nanoparticles with the diameter of up to 10 Å prevails, and the number of large particles is insignificant. Eventually nanoparticles are integrated; therefore the number of particles of small diameter decreases. However, there are larger nanoparticles having the size of more than 20 Å whose formation was not observed at the earlier stages of condensation (Fig. 14).

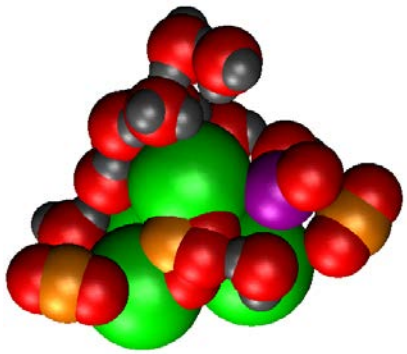

Fig. 14. Image of formed aerosol nanoparticle

VI. Research Results of the Elastic Properties of Nanoparticles and Nanocomposites

Detailed use of the proposed methodology for calculating the deformation parameters of a sample of cesium nanoparticles is discussed below [23, 24]. The number of atoms in nanoparticles ranged from 216 to 200190. Diameter equilibrium nanoparticles with cesium is from 3 nm to 27 nm. The number of atoms is Increased as long as the elastic modulus reaches a value nanoparticles reference value Cs. An important task in the development of nanotechnology in Russia and abroad is to determine the size of the nanoparticles, in which the mechanical characteristics will be the same as the reference values of the macro stuff. Of particular interest to the study of mechanical characteristics of the nanoparticles are "small" size nanostructures with the number of atoms more 10 000.

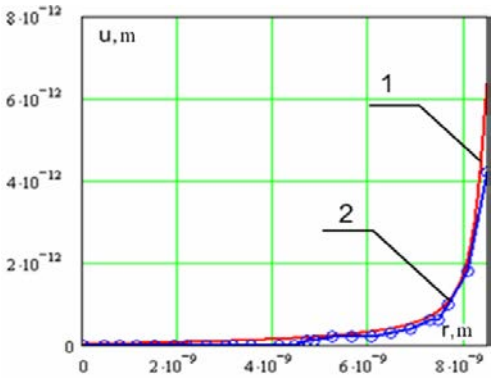

Fig. 15. The dependence of the displacement from the radius: 1 – for elastic ball, 2 – for cesium nanoparticles consisting of 49 995 atoms; $E = 1.73 \cdot 10^9$ Pa – reference value of macro material cesium

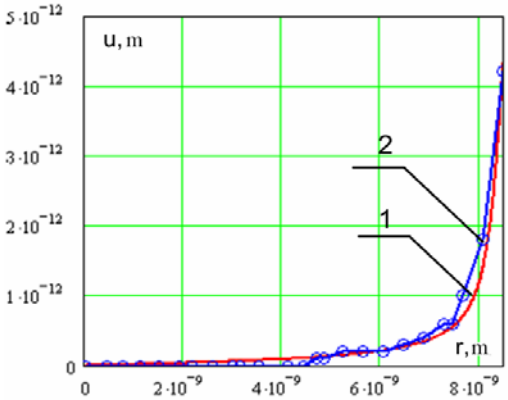

Fig. 16. The dependence of the displacement from the radius: 1 – for elastic ball, 2 – for cesium nanoparticles consisting of 49 995 atoms; $E = 2.5 \cdot 10^9$ Pa – modulus of elasticity of the investigated nanoparticles

Fig. 15 solid line 1, shows the displacement distance along the loading axis to the center of the "equivalent" elastic element reference values modulus cesium. The same graph (Fig.15, line 2) shows the radial displacements of atoms from the distance to the center of mass of nanoparticles r, for constant Poisson's ratio. The graphs show that these dependencies are not identical. Therefore, changing the modulus of elasticity, it is necessary to achieve data fusion curves (Fig. 16), which is the criterion for the minimum mean square error. The mean square error is a pronounced minimum (Fig. 17).

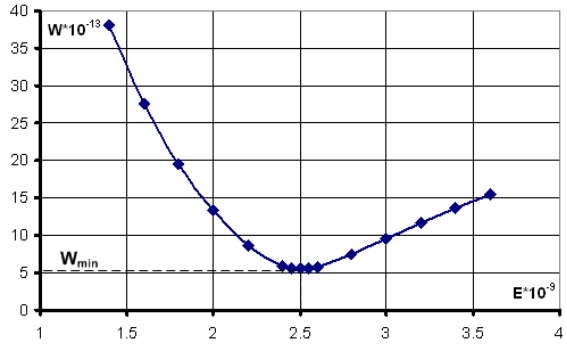

Fig. 17. The dependence of the mean squared error W of the elastic Young's modulus E "equivalent" element, for nanoparticles of cesium (49 995 atoms)

Changing the effective bulk modulus dimensionless inclusions depending on the diameter of the above nanoparticles according to (19) is shown in Fig. 18. Triangular markers are shown the data series of numerical experiments, the results of which was subsequently constructed approximating the trend line. The mathematical expression of the curve approximation allowed to determine unknown coefficients $A = 0.882$ and $B = -1.083$ of the equation (19). The index of the effective bulk modulus indicates the magnitude of Poisson's ratio corresponding to the reference value of cesium.

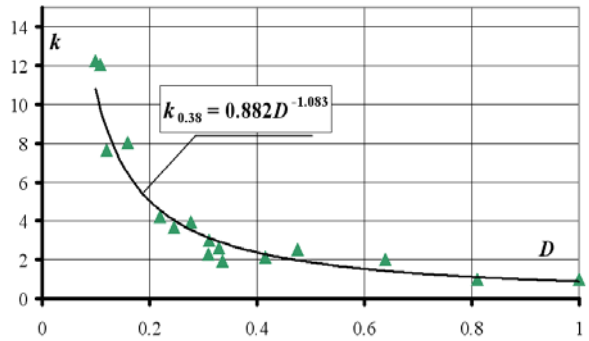

Fig. 18. Changing the dimensionless effective bulk modulus inclusions depending on the dimensionless diameter of inclusions

The mathematical formulation of the curve of the dimensionless bulk modulus of inclusions is the basis for the calculation of the deformation characteristics of composite materials containing nanoparticles. Bulk modulus and shear modulus of the composite depend on the size of the inclusions contained therein. For a composite material consisting of a polystyrene matrix and nanoinclusions cesium dependence of the dimensionless unit of the reduced diameter is shown in Fig. 19.

Analysis of the chart shows that the deformation characteristics are largely dependent on the proportion of the

concentration of nanoparticles in the formed composite. Small nanostructures ($\bar{d} < 0,3$) increase the bulk modulus of the nanocomposite, large nanoparticles ($\bar{d} > 0,3$) lead to its weakening [25, 26].

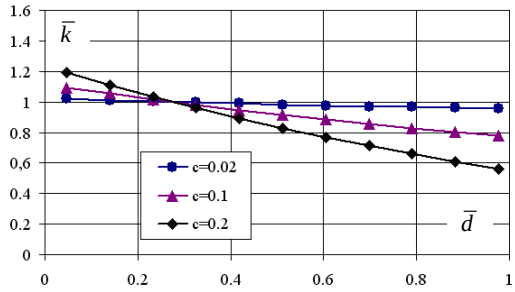

Fig. 19. The dependence of the dimensionless bulk modulus of the nanocomposite of the reduced size contained nanoparticles

Further studies were carried out for the following materials: pure aluminum; aluminum nanocomposite with iron nanoparticles radius of 1 nm; aluminum nanocomposite nanocylinders iron radius of 1 nm. Periodic boundary conditions were used for the simulation. The simulation was performed under standard thermodynamic conditions. The process of destruction of the nanocomposite material with a nanoparticle at time 35 ps, under the influence of tensile forces is shown in Fig. 20.

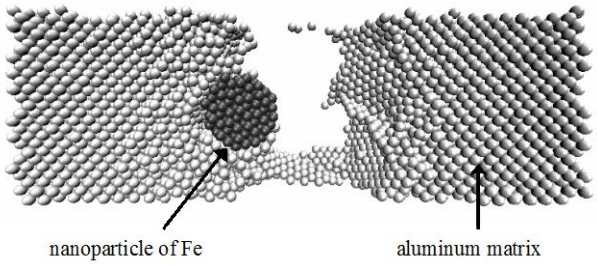

Fig. 20. The process of destruction of the metal nanocomposite at time 35 ps in tension

As can be seen from Fig. 20 restructuring of the atomic structure of the nanocomposite is observed. The destruction occurs gradually. The formation of isthmus is shown. These observations are confirmed by Fig. 21. Stress-strain are given in Fig. 21.

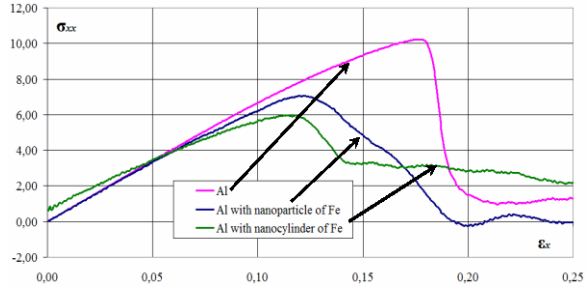

Fig. 21. The stress-strain stretching for a variety of nanocomposite materials

Deformation pattern for the case of composite shear is shown in Fig. 22. The origin of irregularities is observed in the place where the iron nanoparticles. Rebuilding the crystal structure occurs in the matrix material and the material of the nanoparticles. Stress-deformation dependence is shown in Fig. 23 for the case of shear.

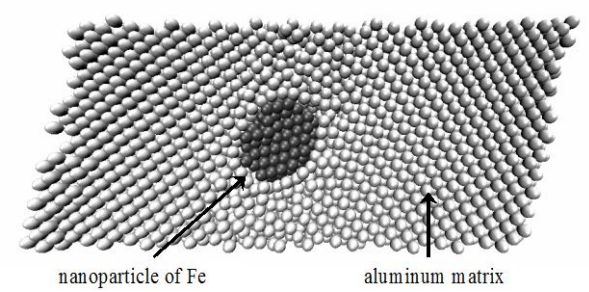

Fig. 22. The process of destruction of the metal nanocomposite at time 35 ps in shear

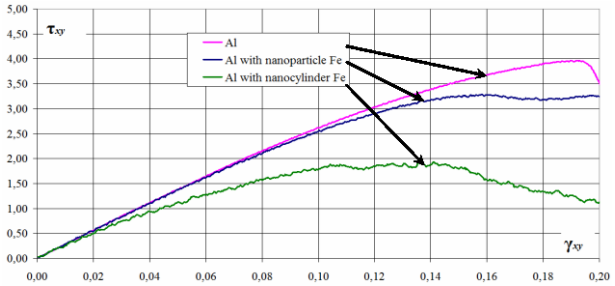

Fig. 23. The stress-strain shearing for a variety of nanocomposite materials

VII. Conclusion

Simulation method of structural, quantitative and deformation properties of nanoparticles, nanoaerosols, and nanocomposites based on them is offered. The model allows to study the dynamic characteristics nanoobjects throughout the life cycle of their use, starting from the processes of formation of nanoparticles and ending its influence on the mechanical parameters of the composite.

Was investigated, that the formation of composite nanoparticles, used to feed crop yields, molecules K_2CO_3, H_2O and MgO are grouped in nanoparticles. Molecules of oxygen, nitrogen and carbon dioxide were remained in the gaseous medium. Condensation nuclei thus are molecules of potassium carbonate.

The problem of condensation of a mixture of aerosol fire extinguishers was solved, during which the equilibrium structure of the molecules of the initial mixture, the composition of the condensable nanoparticles and changes in the thermodynamic characteristics of the system were identified. The changes in the quantitative and dimensional parameters of nanoparticles in the simulation process were investigated.

Calculated dependences of the modulus of elasticity, bulk

modulus of nanoparticles of cesium on their diameter were obtained. Curves were obtained on the basis of matching the solutions of the molecular dynamics and the theory of elasticity, carried by vectors of displacements in points coinciding with the position of the atoms of the nanoparticle. The critical diameter of nanoparticles cesium (21.5 nm) is calculated. If you increase the size of nanostructures is more critical diameter the strength characteristics of nanoparticles coincide with the reference values of the macro materials.

The dependence of the dimensionless effective bulk modulus of nanoparticles cesium is built. Based on this the mathematical formulation of dependence of the effective bulk modulus is given. Formalization of the change in the effective bulk modulus and shear modulus nanoinclusions depending on their size is an important part to determine the deformation properties of nanocomposite materials.

On the example of polystyrene matrix and cesium nanoparticles it is shown that adding nanostructures in the composite can lead to different effects. Hardening of the material is observed at small sizes of nanostructures. The deterioration of the strength characteristics occurs when the nanoparticles have a significant size.

REFERENCES

[1] R. Dingreville, J. Qu, M. "Cherkaoui, "Surface free energy and its effect on the elastic behavior of nano-sized particles, wires and films," *Journal of the Mechanics and Physics of Solids*, vol.53, no.8, pp. 1827-1854, 2004.

[2] Q.-Q. Ni, Y. Fu, M. Iwamoto, "Evaluation of Elastic Modulus of Nano Particles in PMMA/Silica Nanocomposites," *Journal of the Society of Materials Science*, vol.53, no.9, pp. 956-961, 2004.

[3] A.K. Sinha, K. Suzuki, M. Takahara, H. Azuma, T. Nonaka, K. Fukumoto, "Mesostructured Manganese Oxide-Gold Nanoparticle Composites for Extensive Air Purification," *Angewandte Chemie*, vol.119, issue 16, pp. 2949-2952, April 2007.

[4] A.V. Korenevsky, V.V. Solrokin, G.I. Karavaiko, "The interaction of silver ions with the cells of Candida utilis," *Microbiology*, vol.62, no.6, pp. 1085-1092, 1993.

[5] H.H.K. Xu, M.D. Weir, L. Sun, S. Takagi, and L.C. Chow, "Effects of calcium phosphate nanoparticles on Ca-PO_4 composite," *J. Dent Res.*, vol.86(4), pp. 378-383, 2007.

[6] Q.M. Chermont, C. Chanéac, J. Seguin, F. Pellé, S. Maîtrejean, J.P. Jolivet, D. Gourier, M. Bessodes, D. Scherman, "Nanoprobes with near-infrared persistent luminescence for in vivo imaging," *PNAS*, vol.104, no.22, 2007, pp. 9266-9271.

[7] D. Lee, S. Khaja, J.C. Velasquez-Castano, M. Dasari, C. Sun, J. Petros, W.R. Taylor & N. Murthy, "In vivo imaging of hydrogen peroxide with chemiluminescent nanoparticles," *Nature Materials*, vol.6, pp. 765-769, 2007.

[8] M.R. Choi, K.J. Stanton-Maxey, J.K. Stanley, C.S. Levin, R. Bardhan, D. Akin, S. Badve, J. Sturgis, J.P. Robinson, R. Bashir, N.J. Halas, S.E. Clare, "A Cellular Trojan Horse for Delivery of Therapeutic Nanoparticles into Tumors," *Nano Lett.*, vol.7, pp. 3759-3765, 2007.

[9] A.L. Stepanov, V.N. Popok, D.L. Hole, A.A. Bukharaev, "The interaction of high-power laser pulses with glasses containing implanted metal nanoparticles," *Solid State Physics*, vol.43, issue 11, pp. 2100-2106, 2001.

[10] T. Delclos, C. Aimé, E. Pouget, A. Brizard, I. Huc, M.H. Delville, R. Oda, "Individualized Silica Nanohelices and Nanotubes: Tuning Inorganic Nanostructures Using Lipidic Self-Assemblies," *Nano Lett.*, vol.8(7), pp. 1929-1935, 2008.

[11] R. Zhang, L. Fan, Y. Fang and S. Yang, "Electrochemical route to the preparation of highly dispersed composites of ZnO/carbon nanotubes with significantly enhanced electrochemiluminescence from ZnO," *J. Mater. Chem.*, vol.18, pp. 4964-4970, 2008.

[12] A.V Vakhrushev, A.Y. Fedotov, "The study of the formation of composite nanoparticles from the gas phase by mathematical modeling," *Chemical Physics and Mesoscopics*, vol.9, no.4, pp. 333-347, 2007.

[13] A.V. Vakhrushev, A.Y. Fedotov, A.A. Vakhrushev, V.B. Golubchikov, A.V. Givotkov, "Multilevel simulation of the processes of nanoaerosol formation. Part 1. Theory foundations," *International Journal of Nanomechanics Science and Technology*, vol.2, issue 2, pp. 105-132, 2011.

[14] A.V. Vakhrushev, A.Y. Fedotov, A.A. Vakhrushev, V.B. Golubchikov, A.V. Givotkov, "Multilevel simulation of the processes of nanoaerosol formation. Part 2. Numerical investigation of the processes of nanoaerosol formation for suppression of fires," *International Journal of Nanomechanics Science and Technology*, vol.2, issue 3, pp. 205-216, 2011.

[15] A.V. Vakhrushev, A.Y. Fedotov, "Investigation of probability distribution laws of the structural characteristics of nanoparticles, simulated by molecular dynamics," *Computational continuum mechanics*, vol.2, no.2, pp. 14-21, 2009.

[16] M.I. Baskes, "Modified embedded-atom potentials for cubic materials and impurities," *Phys. Rev. B*, vol.46, no.5, pp. 2727-2742, 1992.

[17] C.E. Carlton, P.J. Ferreira, "What is behind the inverse Hall–Petch effect in nanocrystalline materials," *Acta Materialia*, vol.55, pp. 3749-3756, 2007.

[18] R.M. Christensen, Mechanics of composite materials," J. Wiley, 2nd ed., New York, p. 348, 1979.

[19] A.V. Vakhrushev, A.Y. Fedotov, A.A. Vakhrushev, V.B. Golubchikov, A.V. Givotkov, "Multilevel simulation of the processes of nanoaerosol formation. Part 3. Numerical investigations of nanoaerosols for feeding plants from the gas phase," *International Journal of Nanomechanics Science and Technology*, vol.2, issue 4, pp. 309-322, 2011.

[20] A.V. Vakhrushev, V.N. Alikin, V.B. Golubchikov, A.Y. Fedotov, "Nanobiotechnology of growing plants," *Nanotechnology Ecology Manufacturing*, no.1, pp. 108-112, 2009.

[21] A.V. Vakhrushev, A.Y. Fedotov, "Multilevel mathematical modeling of the condensation processes in the aerosol nanosystems," *Alternative Energy and Ecology*, no.8, pp. 8-21, 2014.

[22] A.V. Vakhrushev, V.B. Golubchikov, A.Y. Fedotov, A.V. Zhivotkov, "Multilevel modeling of condensation of molecular mixtures in aerosol fire extinguishers," *Chemical Physics and Mesoscopics*, vol.13, no.43 pp. 340-350, 2011.

[23] A.V. Vakhrushev, A.Y. Fedotov, A.A. Shushkov, "Calculation of Elastic Properties of Composite Materials Based on Nanoparticles Using Multilevel Modeling," *Advances in Sustainable Petroleum Engineering Science*, vol.6, issue 3, pp. 283-298, 2014.

[24] A.V. Vakhrushev, A.Y. Fedotov, A.A. Vakhrushev, "Modeling of processes of composite nanoparticle formation by the molecular dynamics technique. Part 1. Structure of composite nanoparticles," *International Journal of Nanomechanics Science and Technology*, vol.2, issue 1, pp. 9-38, 2011.

[25] A.V. Vakhrushev, A.Y. Fedotov, A.A. Vakhrushev, "Modeling of processes of composite nanoparticle formation by the molecular dynamics technique. Part 2. Probabilistic laws of nanoparticle characteristics," *International Journal of Nanomechanics Science and Technology*, vol. 2, issue 1, pp. 39-54, 2011.

[26] A.V. Vakhrushev, A.Y. Fedotov, A.A. Vakhrushev, A.A. Shushkov, A.V. Shushkov, "The study of mechanisms of formation of metal nanoparticles, mechanical and structural characteristics of nanoparticles and composites based on them," *Chemical Physics and Mesoscopics*, vol.12, no.4 pp. 486-495, 2010.